VISCOELASTIC RELAXATION OF

NEWSPRINT IN WOUND ROLLS

By

SAMUEL DAVID PRICE

Bachelor of Science

Oklahoma State University

Stillwater, Oklahoma

1995

Submitted to the Faculty of the
Graduate College of
Oklahoma State University
in partial fulfillment of
the requirements for
the degree of
MASTER OF SCIENCE
December, 1996

VISCOELASTIC RELAXATION OF

NEWSPRINT IN WOUND ROLLS

Thesis Approved:

_____
Thesis Advisor

_____

_____
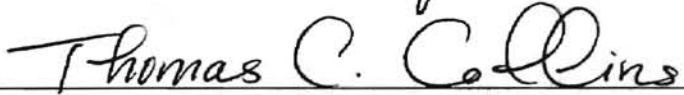
_____
Dean of Graduate College

ii

ACKNOWLEDGMENTS

Without the guidance and advice from Dr. J. Keith Good I could not have completed this work. I would not have been granted this opportunity without his trust and faith, and for that I am truly grateful. This has been the most rewarding and educational experience I have ever had.

Dr. Eric Price gave me a position in which I could affect the lives of my fellow students. It is not easy to teach. I would like to thank Dr. Price for the experience that has made me a more compassionate and articulate student.

I am, of course, grateful for the advice and leadership of the committee members, who lent me their expertise to improve this thesis.

I am indebted to all those whom I worked with during this research. They provided me with direction and escape from the pressures of work.

Lastly, and most importantly, I would like to thank my wife. She understood and supported me through late nights and long hours. The journeys we take we take together, in love, and hand in hand. This work I dedicate to you, Angela, my love, my life, without which this would all be meaningless.

TABLE OF CONTENTS

LIST OF TABLES

LIST OF FIGURES

NOMENCLATURE

c	Coefficient of viscosity, s-psi
E	Elastic Modulus
E_c	Core modulus, psi
E_r	Radial modulus, psi
E_θ	Circumferential modulus, psi
J	Creep compliance, 1/psi
J(t)	Creep compliance as a function of time, 1/psi
$J_0, J_1 \ldots J_n$	Creep compliance constants of generalized Maxwell model, 1/psi
J_r	Radial creep compliance, 1/psi
J_θ	Circumferential creep compliance, 1/psi
$J_{\theta r}, J_{r\theta}$	Cross direction creep compliance, 1/psi
P	Pressure, psi
r	Roll radius, inch
r_{in}	Inner roll radius, inch
r_{out}	Outer roll radius, inch
T_w	Winding stress, psi
t	Time
$\varepsilon(t)$	Creep, time dependent strain, in/in

ε	Strain in/in
σ_0	Initial stress, psi
σ	Stress, psi
σ_r	Radial Stress, psi
$\Delta\sigma_r$	Change in Radial Stress from t_i to t_{i+1},psi
η_1	Viscosity, s-psi
τ	Relaxation time, s
ν	Poisson's ratio
μ	Coefficient of friction

CHAPTER 1

INTRODUCTION

Web materials include paper, plastic, metal and cloth. Products such as film, tape, clothing, paper, foil, etc. were all webs at some point in their processing. Webs have the same basic properties in common: (1) they are thin, (2) they are continuous in that they can be wound onto rolls and (3) they will not support bending.

Web handling is the science and engineering behind the processing of web materials. Typical web handling operations include slitting, or cutting the web into smaller widths, coating, drying, winding and transportation. Profits may be improved by eliminating defects and product losses that may occur during any one of these processes.

Winding is the process of spinning the web into a spiral onto a hollow tube called a core. Cores can be made of paper, wood, metal, plastics or composite materials. The type of core used depends on the stresses the web may experience. There are two main types of winding: constant torque centerwinding and surface winding. As the name implies, constant torque centerwinding means that the roll is wound by powering a shaft through the core, i.e. the center of the roll, with constant torque. Surface winding is achieved by winding the roll via a nip roll turning on the surface of the winding roll (Figure 1.1). The force at which the nip presses into the roll is the nip load, F.
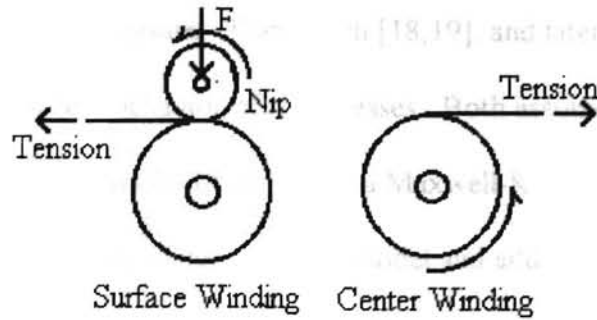
Figure 1.1. Types of Winding.

Winding technique directly affects roll quality. A superior wound roll is one that is free of defects and resists the formation of defects. A roll damaged by defects like tears, wrinkles, buckles or scratches must either be re-coated, rewound or destroyed. The source of defects may be the web itself, processing (coating, slitting, etc.), winding, post winding operations or even storage. Winder related defects can be prevented with the proper combinations of torque, speed, tension and nip loads.

Historically, the choice of winding parameters (torque, speed, tension, etc.) has been empirically based. Today educated choices use winding models to determine these parameters. Given the material properties for the web and core plus the winding conditions, a model can predict the radial and circumferential stresses in the roll. Gutterman [6] began the analysis of wound roll stresses in the late 1950's. Altmann [1], assuming homogeneous and anisotropic web properties throughout the roll, presented an analytical solution for the stress distributions in the wound roll. Yagoda [22] accounted for core deformation by correctly applying the inner boundary condition. Pfeiffer [10,11,12] formulated an energy solution that employed a radial modulus which was

2

linearly dependent on radial pressure. Tramposch [18,19], and later Lin and Westmann [9], investigated the transient behavior of roll stresses. Both assumed isotropic viscoelastic materials. Tramposch [18,19] chose a Maxwell-Kelvin constitutive law. Lin and Westmann [9] chose a generalized Maxwell model and added to Tramposch's work by accounting for winding time in the analysis. Following was Hakiel's elasticity model [7] for wound rolls. The Hakiel model requires a numerical solution to update the radial modulus as winding progresses. Qualls' [13] model predicts the orthotropic viscoelastic behavior of the wound roll and its response to temperature changes.

Qualls presented his model in a program known as Viscowinder and verified it using low density polyethylene. The objective of this research is to study the versatility of Viscowinder, and hence Qualls' model, by applying it to rolls of newsprint.

This work will complement work done by Qualls and thus will apply only to center wound rolls. In as such, the same assumptions apply: (1) axisymmetric roll body, (2) circumferential changes in geometry, properties or stresses are ignored and (3) the rolls are two-dimensional rolls. Hence, radial and circumferential stresses are assumed to be a function of radius only. Width wise variations in caliper or tension are assumed to have no effect on the predicted stress distributions.

This work is both important and useful in that it begins the work of widening the transient roll analysis to other media. It initiates investigations into the hygroscopic effects on viscoelastic response in paper products.

CHAPTER 2

BACKGROUND

Viscoelasticity and Viscoelastic Materials

Upon loading, viscoelastic materials first experience elastic deformation, followed by a slow and continuous increase in strain at a decreasing rate. When the load is removed, the material initially recovers elastically and then experiences a continuously decreasing strain to a finite limit.

Creep is the time-dependent strain of a viscoelastic material under constant stress (Figure 2.1). Creep experiments are often done under constant load, even when the cross-sectional area is changing. For small strains, constant load and constant creep experiments are the same, because the change in cross-sectional area is negligible. The creep tests performed in this thesis were constant load experiments. Typically, a weight is applied at time zero by hand. There are various means to measure the deformation due to the applied load. One of the easiest to use is the linear variable differential transducer (LVDT). Data acquisition software (Labtech notebook) can then be connected to the LVDT to enable continuous unsupervised measurements. The voltage data can be converted to strain data with the aid of a spreadsheet program like EXCEL. The strain

4
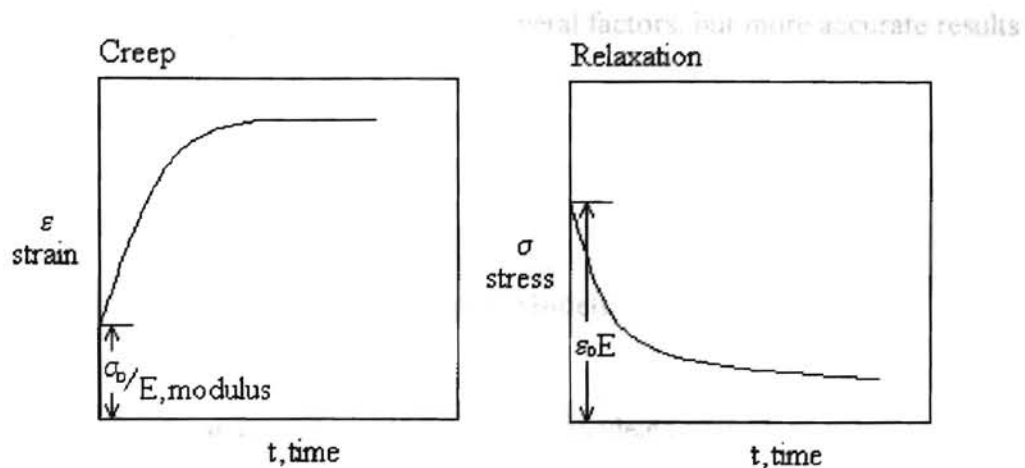
Figure 2.1. Creep and Relaxation.

can then be converted into the various forms, like creep compliance, required by Viscowinder.

Relaxation is the stress response of a material to a step strain input. Initially, stress is a maximum. As time progresses, the stress in the material decreases, or relaxes, at a decreasing rate. Creep and relaxation experiments contain the same information, but strain measurements are easier to control, cost less and are more accurately performed.

For a material to be considered linearly viscoelastic, stress must be proportional to strain at a given time and the linear superposition principle must hold. These requirements are stated mathematically below:

$$\varepsilon[c\sigma(t)] = c\varepsilon[\sigma(t)] \qquad (2.1)$$

$$\varepsilon[\sigma_1(t) + \sigma_2(t - t_1)] = \varepsilon[\sigma_1(t)] + \varepsilon[\sigma_2(t - t_1)] \qquad (2.2)$$

Most materials are linear over certain ranges of time, stress, strain, temperature and/or humidity and are nonlinear over a larger range of these variables. The use of linear

5

viscoelastic constituent Equations depends on several factors, but more accurate results are achieved by using nonlinear viscoelastic theory.

Viscoelastic Models

Historically, linear viscoelastic behavior was modeled with various combinations of linear springs and dashpots. The simplest models used one spring and one dashpot. Maxwell connected the spring and damper in series, whereas Kelvin connected the two in parallel. Figure 2.2 shows the two basic models, along with their creep response and creep functions due to a step change in stress and the removal of that stress at time t1.

Subsequent models involved series and/or parallel combinations of Kelvin and/or Maxwell models. A Maxwell model connected in series to a Kelvin model is known as the Burgess model. Figure 2.3 shows the creep response of the Burgess model to a step change in stress and the relaxation response after the stress is removed at time t1.

Another important combination model is the generalized Maxwell model. Simply put, it is the series or parallel connection of N number of Maxwell models. A two time constant generalized Maxwell model appears below, represented mathematically with the creep compliance constants, J. Creep compliance is the time dependent strain, $\varepsilon(t)$, divided by the constant initial stress, σ_0.

$$J(t) = J_0 + J_1 e^{\frac{-t}{\tau_1}} + J_2 e^{\frac{-t}{\tau_2}} \tag{2.3}$$

σ=stress ε=strain

Kelvin

$\varepsilon(t)= \sigma_0/E(1- e^{(-Et/c)})$

E modulus

c coefficient of viscosity

Maxwell

$\varepsilon(t)= \sigma_0/E + t\sigma_0/c$
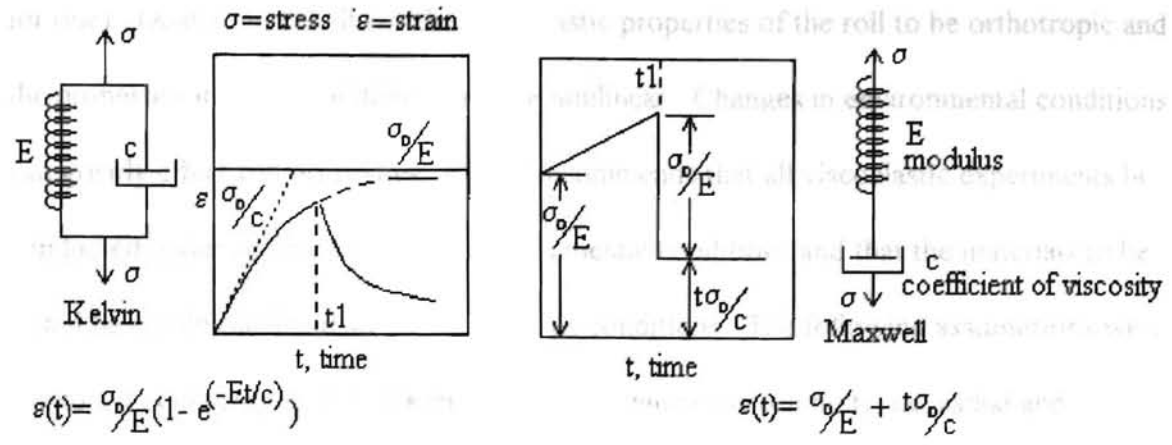
Figure 2.2. Kelvin and Maxwell Models of Viscoelasticity.

$\varepsilon(t)= \sigma_0/E(1- e^{(-Et/c)}) + \sigma_0/E + t\sigma_0/c$

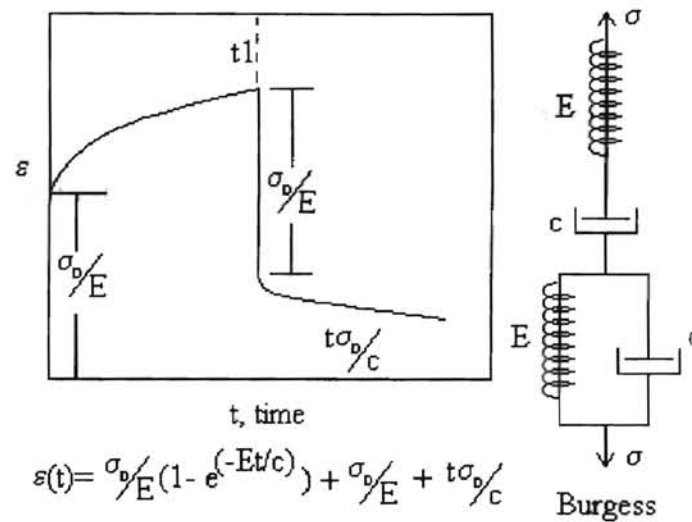Burgess

Figure 2.3. Burgess Viscoelastic Model.

Qualls [13] chose the general Maxwell model with series elements for the following reasons: (1) it allows for instantaneous elastic deformations, and (2) a general constituent model must be chosen if a wide variety of materials can be utilized (newsprint,

7

for one). Qualls' model allows the viscoelastic properties of the roll to be orthotropic and the properties in the radial direction to be nonlinear. Changes in environmental conditions can greatly effect roll properties. Qualls recommends that all viscoelastic experiments be conducted under accurately known environmental conditions and that the materials to be tested be conditioned and stored at the same conditions. The following assumptions were employed in development of the model: (1) axisymmetric roll body, i.e. radial and circumferential stresses, are a function of radius only, (2) circumferential changes in geometry, properties or stresses are ignored and (3) the roll can be modeled as two-dimensional with unit width; in other words, width-wise variations in caliper or tension will have no effect on the predicted stress distributions. Poisson terms are commonly ignored in web modeling because they are either zero or are small compared to unity. Qualls' model makes the same assumption but adds that in the generalized Maxwell model $J_{\theta r}$ and $J_{r\theta}$ are equal and can be related to J_θ by:

$$J_{\theta r} \equiv -\nu J_\theta \tag{2.4}$$

Qualls' model is presented below.

$$\int_0^t [J_\theta(t^*)\frac{\partial}{\partial \tau}(r^2\frac{\partial^2\sigma_r}{\partial r^2}) + \{3J_\theta(t^*) + J_{\theta r}(t^*) - J_{r\theta}(t^*) + r\frac{\partial}{\partial r}J_\theta(t^*)\}\frac{\partial}{\partial \tau}(r\frac{\partial\sigma_r}{\partial r}) +$$

$$\{r\frac{\partial}{\partial r}(J_\theta(t^*) + J_{\theta r}(t^*)) + J_\theta(t^*) + J_{\theta r}(t^*) - J_r(t^*) - J_{r\theta}(t^*)\}\frac{\partial\sigma_r}{\partial \tau}]d\tau \tag{2.5}$$

where $t^* = t - t'$. The variable t', the variable of integration, is the time that an infinitesimal step change in stress in applied to the web.

Qualls arrived at this second order partial differential Equation by modeling the winding process as the addition of pretensioned concentric hoops of web material onto a compliant core. The stresses are incrementally changed as each new layer is added to the

8

roll. Assuming the wound roll is axisymmetric dictates that the stresses, strains and displacements are functions of roll radius only. His governing Equations in polar coordinates are:

Equilibrium Equation:

$$r\frac{\partial \sigma_r}{\partial r} + \sigma_r - \sigma_\theta = 0 \tag{2.6}$$

Strain Compatibility Equation:

$$r\frac{\partial \varepsilon_\theta}{\partial r} + \varepsilon_\theta - \varepsilon_r = 0 \tag{2.7}$$

Strain-Displacement Relation:

$$\varepsilon_r = \frac{\partial u}{\partial r} \qquad\qquad \varepsilon_\theta = \frac{u}{r} \tag{2.8}$$

where u is the deformation of the web material.

Viscoelastic Constitutive Equations:

$$\varepsilon_r = \int_0^t [J_r(t^*)\frac{\partial \sigma_r}{\partial t'} + J_{r\theta}(t^*)\frac{\partial \sigma_\theta}{\partial t'}]dt' \tag{2.9}$$

$$\varepsilon_\theta = \int_0^t [J_\theta(t^*)\frac{\partial \sigma_\theta}{\partial t'} + J_{\theta r}(t^*)\frac{\partial \sigma_r}{\partial t'}]dt' \tag{2.10}$$

First σ_θ, the circumferential stress, is eliminated by solving Equation (2.6) for σ_θ and substituting the result into Equations (2.9) and (2.10). The two resulting Equations, describing the radial strain, ε_r and the circumferential strain ε_θ, are substituted into the compatibility Equation (2.7). This results in Equation (2.5).

The solution to this second order partial differential boundary value problem was done numerically. The numerical solution method is presented here as the internals of

Viscowinder. Qualls chose the generalized Maxwell model to represent viscoelastic

behavior and, as such, the creep compliance becomes:

$$J(t) = J_0 + \sum_{i=1}^{N} J_i e^{-(t^*)/\tau_i}$$

(2.11)

This choice allows for instantaneous deformation followed by time dependent

deformation, creep, when subject to a change in stress. For an orthotropic material the

creep compliance in the radial, J_r and in the circumferential, J_θ directions must be

independently defined. Additionally, Hakiel [7] and Pfeiffer [10,11,12] have shown that

radial modulus is a function of interlayer pressure. Consequently, the J_0 term of J_r must

also be a function of radial stress. Applying the finite difference solution method to

Equation (2.5) results in:

$$(F_1(r)\frac{r_i^2}{h^2} + F_2(r)\frac{r_i}{2h})\Delta\sigma_{r(i+1)} + (F_3(r) - 2F_1(r)\frac{r_i^2}{h^2})\Delta\sigma_{r(i)}$$
$$+ (F_1(r)\frac{r_i^2}{h^2} - F_2(r)\frac{r_i}{2h})\Delta\sigma_{r(i-1)} + F_4(r) = 0$$

(2.12)

When the boundary conditions are applied, a tri-diagonal system of Equations is

produced and solved by Gaussian elimination for the change in radial stress, $\Delta\sigma_{r(i)}$, at the

current time step. The inner boundary condition provides continuity between core

deformation and the inside of the roll. The outer boundary condition is developed by

taking the strain to be constant and equal to the winding stress multiplied by the

circumferential creep function evaluated at time zero. The deformation of the outside

radius due to changes in stress of the underlying layers is taken to be negligible.

10

Properties of Cellulose Materials

Paper is composed of the wood polymers cellulose, hemicellulose, and lignin. Paper fibers are composed of semicrystalline cellulose in the form of fibrils in a matrix of hemicellulose and lignin. The cell wall of the fiber consists of three layers. Each layer contains fibrils at different orientations to the fiber axis. The largest, and therefore the layer that dominates mechanical properties, is the center layer [15]. Moisture lowers the wood polymers' glass-transition temperature [15,16] which, in turn, effects the mechanical, hygroscopic and creep properties of paper [14,15,16]. Temperature changes effect mechanical properties in two ways: (1) a temperature change alone causes shifts in strength, creep and moduli, and (2) moisture content (at any given relative humidity) decreases with increasing temperature. Moisture and temperature are somewhat interchangeable in their effects on paper properties [14,15]. A temperature increase of as much as 100°C leads to an expansion in the thickness direction equivalent to the dimensional change of paper when its moisture content is increased by only 1%. These changes in geometry cause web buckling and warping. Moisture effects paper cores; for example, doubling the moisture content can half the strength of a paper core [14].

The amount of moisture present effects the material by interfering with interaction forces between polymer chains, thereby increasing their mobility. For the wood polymer, the glass-transition temperature is the most characteristic parameter of the material. At the glass-transition temperature, the material undergoes a substantial drop in elastic modulus and an increase in hygroexpansivity [14,15,16].

11

The higher the density of paper the greater the hygroexpansivity, presumably because the cross fiber expansion pushes the fibers apart in the thickness direction. The elastic modulus is effected by both temperature and moisture content. As temperature or moisture content increases, the elastic modulus decreases. An increase in temperature, though, shifts the softening region to a lower moisture content. In principle, the view of water as a softener is compatible with plasticizing of polymers. Softening also causes elongation and creep to increase [15,16].

Mechanical properties are effected to a larger extent during changing environmental conditions (i.e., cyclic humidity) [3,8,15,20,21] than would be anticipated under equilibrium conditions [2]. This means that there will be a much higher creep rate, a lower elastic modulus and an increased hygroexpansion during non-equilibrium conditions. Byrd and Haslach [3,8] speculate as to the mechanism of accelerated creep.

Cyclic relative humidity produced, among other things, increased fibril angle (of the center layer). The fibril angle is the angle between the fiber axis and the fibril. As the fibril angle increases, the fiber expands. The increase in creep rate under cyclic relative humidity is attributed to interfiber bond rupture. Under constant relative humidity (RH) sheet thickness first increased and then decreased; however, during cyclic RH the sample's thickness continued to increase. Individual fiber perimeters changed as an indirect result of bond breakage. This change in perimeter led to the continued increase of paper thickness. Both tensile strength and elastic modulus initially increased to a maximum value and then decreased to near their original values. Interfiber bonds are being broken during creep. However, the remaining bonds support the load until a critical number of bonds are broken. The support bonds gain added strength during the drying portion of the

cycle due to tensile restraint (dried in stresses) [3]. Haslach [8] builds upon this by incorporating supermolecular motions into the hypothesis.

Generation of free volume is greater in materials undergoing cyclic creep. Free volume is empty space in the amorphous region of the fiber. When the relative humidity is constant, no new free volume is generated or destroyed. Free volume is generated when moisture is adsorbed into the amorphous region of the polymer. Adsorption is an exothermic process driving the temperature out of equilibrium. The generation of free volume allows transverse fiber swelling. However, moisture accelerated creep only occurs in materials whose fibers are anisotropic. The transverse swelling dominates the tensile force in cyclic relative humidity, but the tensile force dominates during constant relative humidity. Microcompression occurs at the interfiber bonds due to the transverse swelling. These microcompressions cause delayed elasticity. Interfiber bonds are broken during creep. However, during constant relative humidity "un-bonding" is due to an increase in total area (by fiber lengthening) and not as a result of the removal of microcompressions. During cyclic creep the microcompressions reform as relative humidity decreases.

Non-equilibrium effects only appear in complex structural materials and are most pronounced in compression. This is thought to be related to dried-in tensile stresses. As the moisture content increases, interfiber bond slippage occurs (due to lowering of glass-transition temperature), which releases the dried-in stresses (contracting the fibers) [15].

Dried-in stresses reduce the paper's hygroexpansivity, but uncontrolled releasing of these stresses causes problems, such as the uneven release of stresses during the storage of wound paper rolls [15].

Related Studies on Creep and Viscoelasticity of Paper

Brezinski [2] states that creep in paper at constant relative humidity is a function of sheet and fiber properties. This is demonstrated by two distinct creep stages. In the first stage, creep is defined by an exponential form:

$$\frac{y}{L_0} = Bt^a + C \qquad (2.13)$$

where y is the total first stage creep deformation, L_0 is the initial span length and t is time. The letters a, B and C are constants.

During increased loading or loading time the second stage creep dominates and the deformation form is logarithmic:

$$\frac{y}{L_0} = K \log t + C' \qquad (2.14)$$

where K and C' are constants. K divided by the initial stress and multiplied by the initial length was found to be constant. C' is mathematically equivalent to the immediate elastic deformation.

One effect of increasing the load is speeding up the response to stress; thus, with higher loading, creep stage two dominates. As loading decreases, the effect of stage one is more pronounced. In first stage creep most of the deformation can be recovered. Conversely, during second stage creep most of the deformation cannot be recovered. In general, increasing the relative humidity increases the total deformation.

Newsprint is highly compressible in the radial direction. As a result, newsprint experiences tension loss. Low density polyethylene (LDPE) that Qualls used to verify his model does not experience this phenomenon. Consequently, adjustments were made to account for tension loss in newsprint.

Tension loss is the loss of wound on tension due to the deformation of the roll as each new layer is being added. Tension loss usually occurs in center winding of web materials that are highly compressible in the radial direction. Newsprint and bond fall in this category along with films or tissues that have high surface roughness [5].

All of the winding models mentioned previously assume that the web tension, T_w, is equivalent to the wound on tension in the outer layer. The radial stress, σ_r, beneath the outer lap is calculated as:

$$\sigma_r = T_w * h/s \tag{2.15}$$

where h is the web caliper and s is the nominal radius of the outer layer. Equation (2.15) is equivalent to the thin walled pressure vessel hoop stress Equation in which T_w is the hoop stress and σ_r is the internal pressure. This Equation assumes that the radial deformations do not affect the internal pressure. However, as the web contacts the winding roll, a large amount of radial strain occurs causing the internal pressure to deform inward. Thus, the resulting interlayer pressure is less than prescribed by Equation (2.15). This is analogous to two cylindrical pieces that are press fit together. If the inner cylinder

should somehow experience a decrease in its outer diameter (such as cooling), then the pressure at the interface between the two cylinders will decrease [5].

Modeling the tension loss is accomplished by modifying Hakiel's model via the following Equation [5]:

$$\text{Wound on Tension} = T_w + E_\theta * u/s \qquad (2.16)$$

This model can then be used to correctly apply the wound on tension as the winding tension in Qualls' program, Viscowinder.

CHAPTER 3

VISCOELASTIC ANALYSIS OF A WOUND ROLL

Experimental Verification

Since paper and many other viscoelastic materials are influenced by variations in temperature and relative humidity, all creep measurements were performed in an environmental chamber. To ensure proper material properties all test specimens were conditioned for 24 hours prior to testing. The environmental chamber allowed for close control of temperature ($\pm 0.1°F$) and humidity ($\pm 1\%$). All tests were performed at 72°F and 45%RH. These conditions nearly matched the newsprint storage conditions of the facilities (75°F and 50%RH).

Recall that in the generalized Maxwell model creep is utilized in the creep compliance form.

MD,

$$J_\theta = (1/E_\theta + a_\theta) + b_\theta e^{(-t/c\theta)} + d_\theta e^{(-t/e\theta)} \tag{3.1}$$

and in the radial direction,

$$J_r = (1/E_r + a_r) + b_r e^{(-t/cr)} + d_r e^{(-t/er)} \tag{3.2}$$

To apply these relationships to Viscowinder, radial and MD modulus, E_r and E_θ, must be measured. Radial and MD creep tests will be used to determine the creep

17

compliance, J_r and J_θ in both directions. Additionally, the time variant radial pressures within a wound roll will be measured to verify the output of Viscowinder. This chapter presents the method behind and the results for each measurement type.

Material Property Measurements

Web Thickness

Newsprint does not have a uniform thickness so an average thickness was used for the calculations. Thickness was measured in two ways -- pneumatically and with a micrometer. The micrometer method involved a stack of newsprint sheets. The stack was measured in several areas and the readings averaged. The average was then divided by the number of sheets in the stack to find the average sheet thickness. The pneumatic method had an advantage over the mechanical method in that the micrometer tended to flatten the sheets of paper. The pneumatic method positions a head above the surface of the paper using a nozzle flapper device, and an LVDT is used to measure the position of the head, which is a measure of the thickness. A sheet was placed in the device, and thickness readings were taken at several sites. These readings were averaged to get the average sheet thickness. The micrometer method was used to check the pneumatic method. The thickness of newsprint was found to vary between 2.6 - 3.0 mils (a mil is 0.001 inches), and the average thickness was 2.8 mils.

It is not clear how thickness effects the load distribution in paper. Changes in moisture content change the thickness of paper [15,17]. As the moisture increases the

modulus lowers and creep increases [3,8,15]. The fibers swell and the fibril angle changes as a function of moisture content. Byrd [3] implies that, as relative humidity increases, the thickness and strain increase while the modulus and maximum tensile strength decrease (Table 3.1).

RH at which specimens tested (23°C), %	Average Sheet Thickness, in	Modulus of Elasticity, 1000 psi	Maximum Stress, psi	Strain at Failure, %
35	.00594	236	1000	.85
50	.00620	211	848	.92
90	.00626	89.2	384	1.4

Table 3.1. Handsheet Properties at Various Relative Humidity Levels.

Machine Direction Modulus

The elastic modulus of newsprint was measured using an Instron #4202 hydraulic testing unit. A small strain rate, 0.001 in/s, is applied to the web, and the resulting load and displacement is measured up to 3.5 pounds of load (1250 psi). The load and displacement data is then converted into stress and strain with the aid of the spreadsheet program *EXCEL*.

Ten one inch wide by twenty inch long samples were used. Figure 3.1 illustrates how the samples were arranged in the machine. Tongue depressors were wrapped around the ends to minimize slippage in the grips.

Figure 3.2 shows the data from the ten tests along with the straight line fit of these points. Table 3.2 shows the average value and standard deviation for the machine direction modulus. The MD modulus, E_θ, is taken as 454,000 psi.
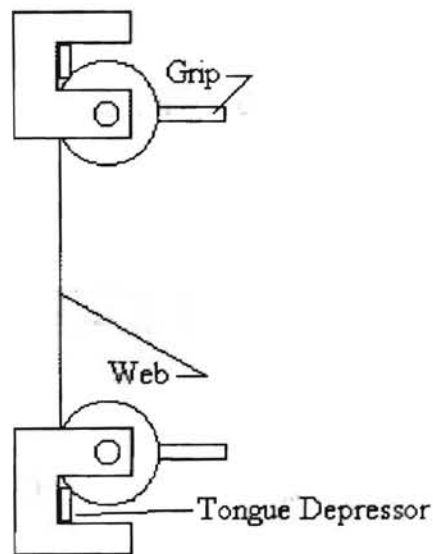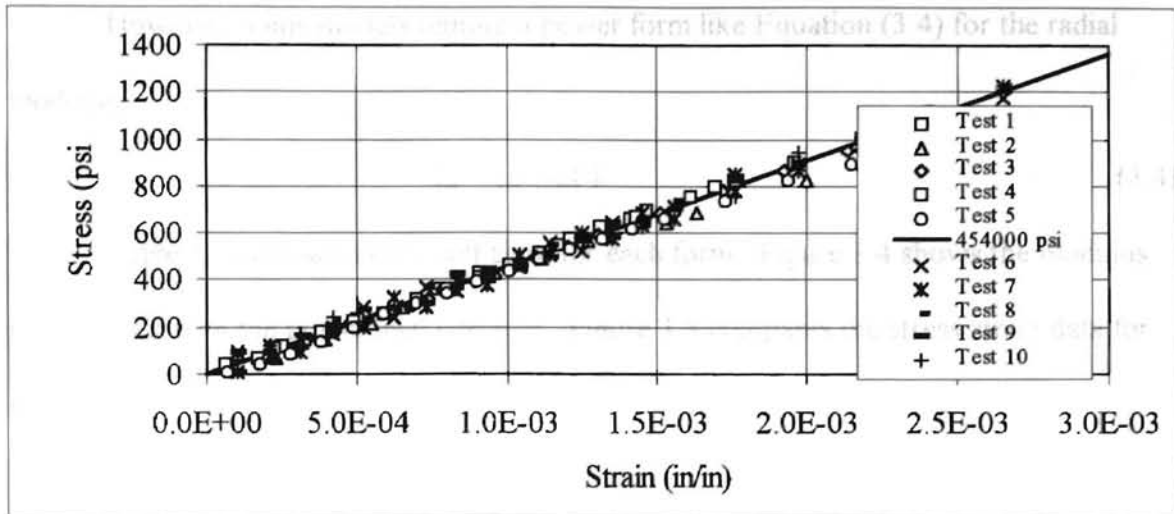

Figure 3.1. Elastic Modulus Setup.

Figure 3.2. MD modulus of Newsprint.

Average	Standard of Deviation
454,000	16,000

Table 3.2. MD modulus of Newsprint.

Radial Modulus

Radial modulus was measured with an Instron #8502 hydraulic tester. Five one inch thick stacks of six by six inch newsprint sheets were used in each test, conditioned as described previously.

Radial modulus is a nonlinear function of pressure. E_r is often fit to a third order polynomial such as Equation (3.3).

$$E_r = aP + bP^2 + cP^3 + d \qquad (3.3)$$

21

However, some models require a power form like Equation (3.4) for the radial modulus.

$$E_r = (a + bP)^c$$ (3.4)

Table 3.3 compares the coefficient for each form. Figure 3.4 shows the modulus data plotted with the polynomial curve fit. Figure 3.3 compares the stress strain data for the five tests.

	a	b	c	d
Coefficient for polynomial form	45.9	-0.365	0.00146	-36.4
Standard Deviation	1.46	0.0583	0.0000372	4.19
Coefficient for power form	0	512	0.719	N/A
Standard Deviation	0	99.3	0.0149	N/A

Table 3.3. Coefficients of Radial Modulus.

Moduli data were measured remotely via Labtech notebook, data acquisition software running on a personal computer. The data was analyzed using the built in EXCEL function LINEST to produce the radial modulus as a function of pressure. LINEST returns the slope of a linear regression through a selected number of data points. This slope is the radial modulus at a particular pressure.
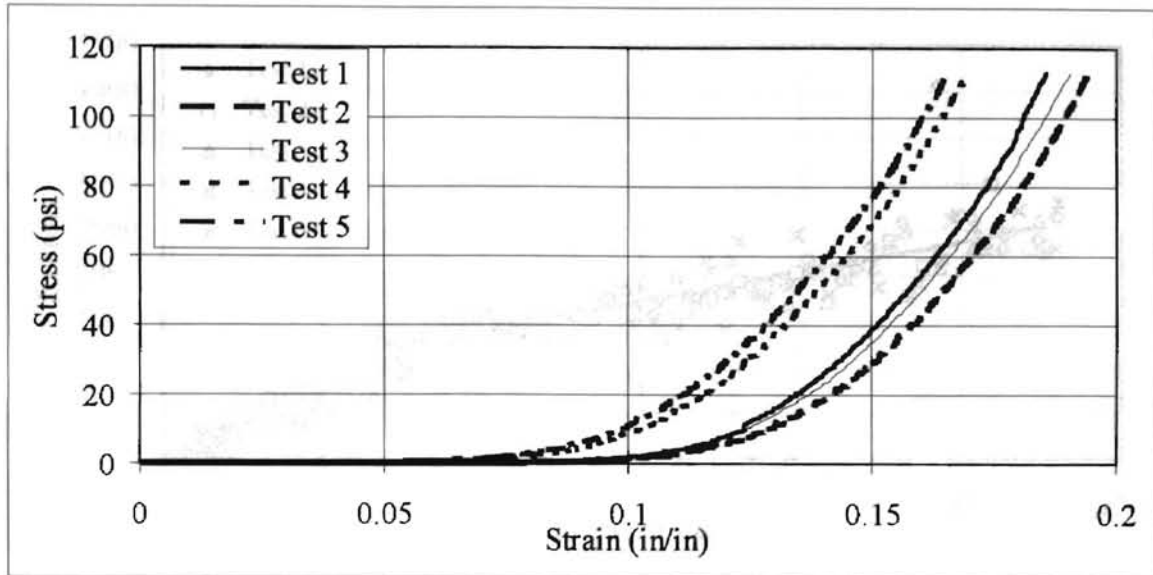
Figure 3.3. Stress vs. Strain in the Radial Direction for Newsprint.

Tension loss is known to occur in newsprint. It is mentioned here because modeling tension loss requires the radial modulus to be determined with high precision, particularly at low pressures. Additionally, the stack must be in the same condition as the outer layer as it contacts the winding roll. The stack is therefore rifled to keep each sheet loose from the next [5]. The separation in Figure 3.3 of each individual stress-strain curve is an indication that tension loss is occurring. Previous compression tests showed this same separation, but the data were not as carefully taken. The E_r data presented in this thesis were taken such that many points were sampled at pressures up to 0.25 psi. This aided a better fit, and thus produced a more precise function for the modulus.
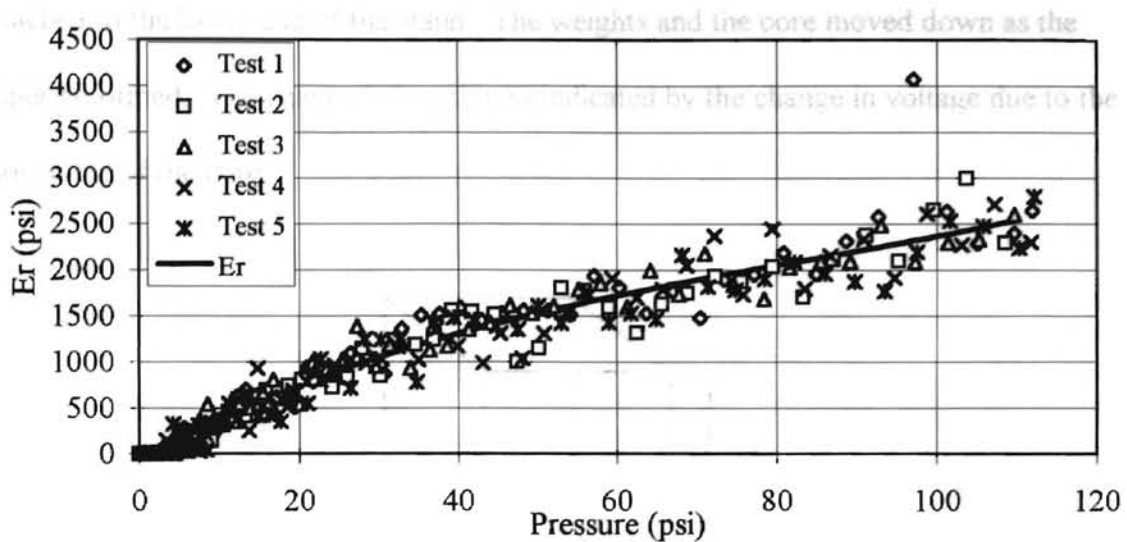
Figure 3.4. Radial Modulus as a Function of Pressure for Newsprint.

Machine Direction Creep Measurements

Three inches wide by twenty inches long newsprint strips were used to find J_θ. The environmental chamber (dimensions, Figure 3.5) enforced a size limit on the samples to be tested. The initial test apparatus only allowed one sample to be tested at a time (Figure 3.6).

The newsprint strip was looped such that the gauge length was 8.5 inches. One and a half inches on each end was carefully marked to provide a gripping surface for the rubber backed aluminum grips. A removable wire was attached to the rod. A hook hanging from the wire held an LVDT core and the weight. The Trans-Tek #0283-000 LVDT is linear over ±0.5 inches, and its sensitivity is 1.903 VAC/Inch/Volt. The aluminum grips were firmly bolted to a stationary experiment stand. The LVDT was

attached to the lower end of the stand. The weights and the core moved down as the paper deformed. The change in length was indicated by the change in voltage due to the movement of the core.
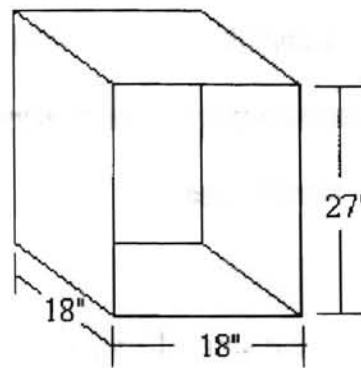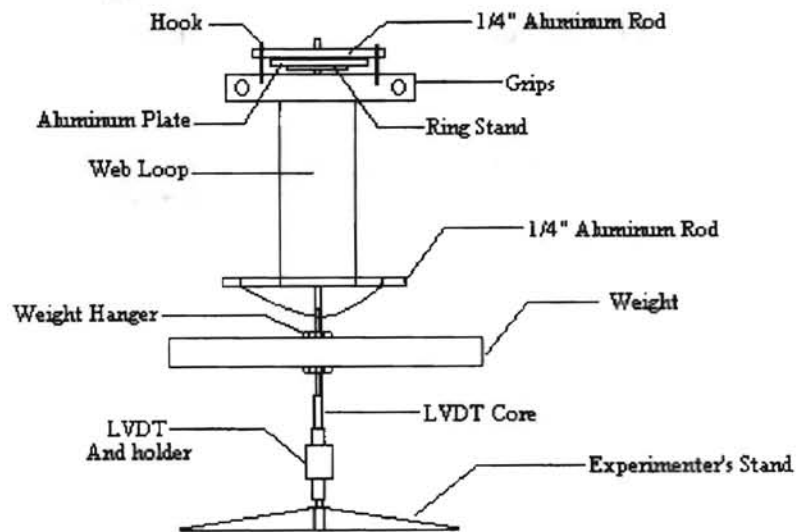

Figure 3.5. Environmental Chamber Dimensions.

Figure 3.6. Initial MD Creep Test Setup.

All creep test data were recorded using Labtech notebook. The first test was run for over a month and showed that after about five days the creep had nearly reached steady-state. As a result, subsequent tests were run for only five days. Figure 3.7 shows the data for this first test compared to the Brezinski form discussed in Chapter 2.

To conserve time, a new test stand was designed and constructed to test as many samples as possible given the environmental chamber's size restraints. It was determined that five samples could be tested simultaneously. Special lead weights had to be cast to accommodate the design.

Figure 3.7 shows test data acquired during this research for a creep test performed on newsprint and a fit of that data in the form of Equation 2.13. The value of a for the test data is 0.21, which is close to Brezinski's value of 0.23.
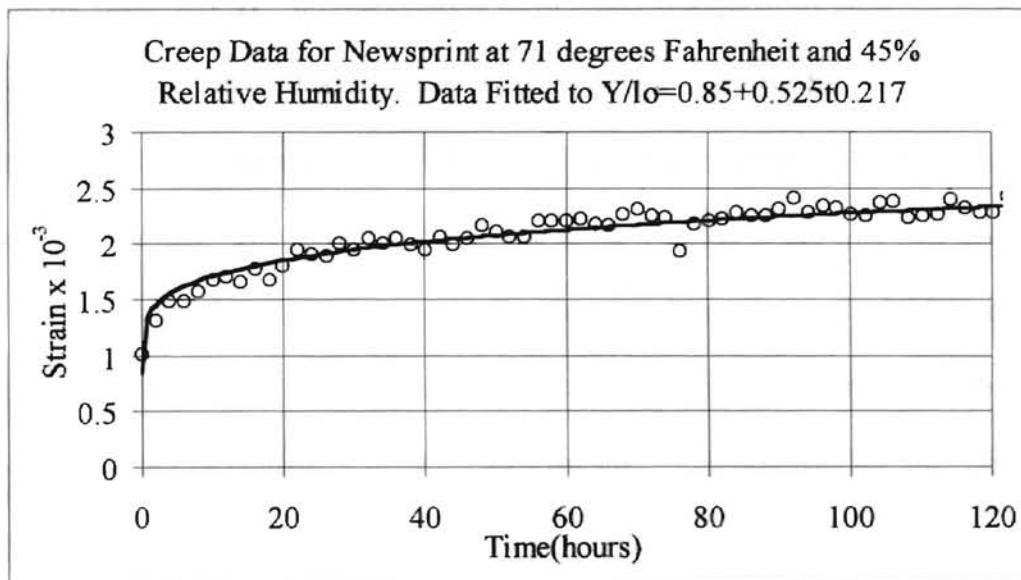

Figure 3.7. MD Creep at 1000 psi.

1.5"x1.5" aluminum angle — Aluminum Grip

5/8" steel bar — Web

Aluminum Rod

Hook

Wire Hanger

Lead Weight

LVDT core with extension rod

LVDT

1/2" aluminum base plate

LVDT core holder attached to base plate
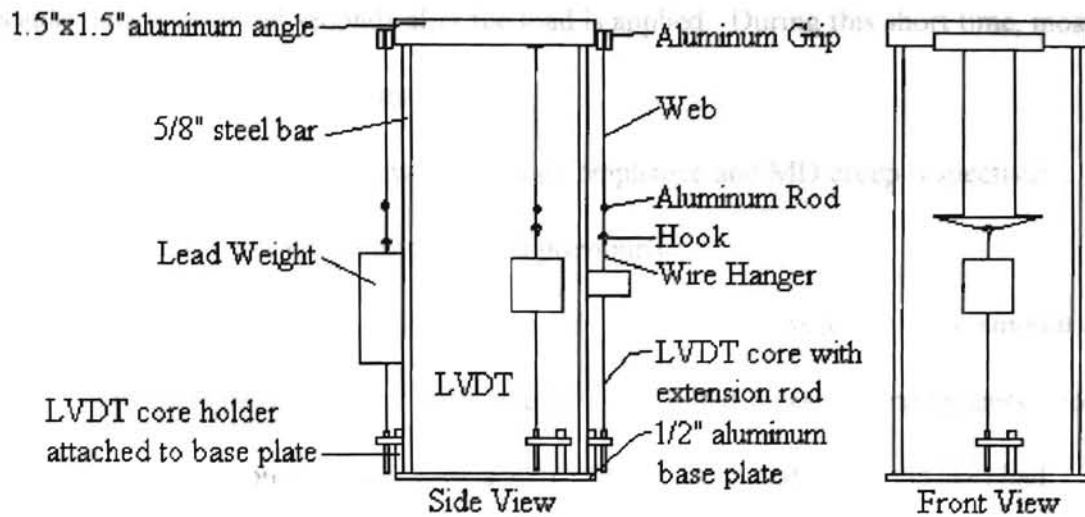
Side View   Front View

Figure 3.8. MD Creep Test Setup For Multiple Initial Stresses.

Three stress levels were investigated, nominally 20, 10 and 5 pounds (1170, 610 and 340 psi respectively). Several samples were tested at each stress level.

Some of the strain measured was due to the applied stress. Some of the strain was the time-dependent portion of strain. The rest of the strain was due to the compliance of the testing apparatus. The compliance was due to the bending of the wire that held the LVDT core and weights. In order to calculate the creep compliance, the initial strain, along with the compliance of the test stand, must be removed. The compliance for the same wire may not be consistent between tests because the position of the wire changes each time the weight is reapplied. Unfortunately, this means that the compliance of the test apparatus is not measurable or predictable. There is a simple solution, however. By subtracting the first data point from all the other data points, both the initial strain and the compliance can be removed from the data. This can be done with some confidence

27

because data is acquired seconds after the load is applied. During this short time, most of the strain is due to elastic deformation.

Figures 3.9 and 3.10 show MD creep compliance and MD creep respectively. The initial strain has been removed as described previously.

Figure 3.10 also indicates some dispersion between stress levels. The amount of dispersion is not significant and is most likely a result of the measurement process. For example, the dispersion in Figure 3.10 is 36% of the average value. Qualls [13] had dispersion that was about 40% of his average value (for LDPE). The dispersion indicates that J_θ was not dependent on stress. As a result, it was a fairly straightforward method to take the average of the creep compliance data (at all pressures) and curve fit the result to find the coefficients of J_θ. Table 3.4 lists the coefficients of the MD creep compliance.
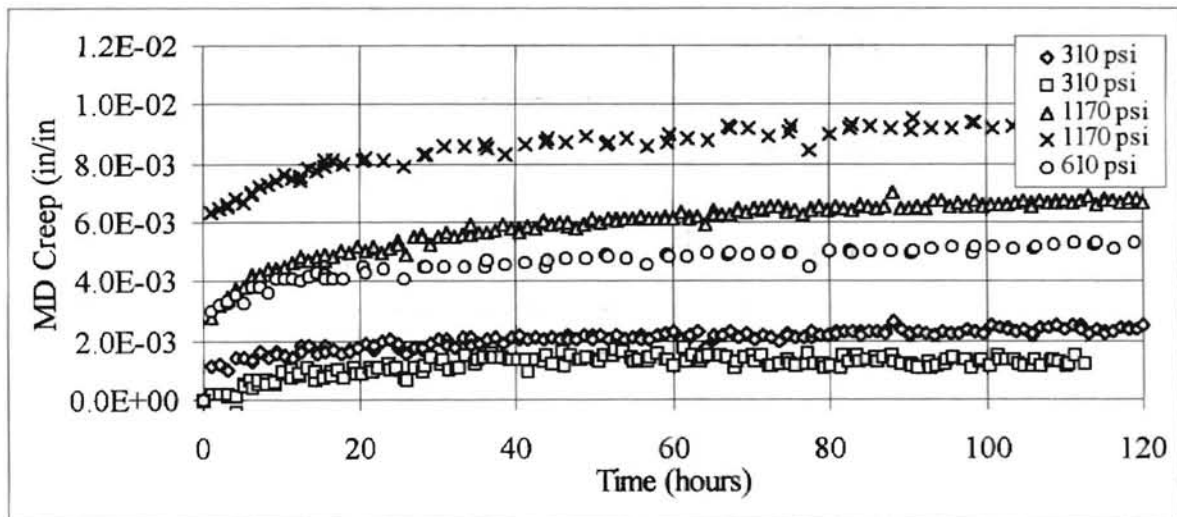

Figure 3.9. MD Creep of Newsprint at 72°F and 45%RH for Various Stress Levels.

28
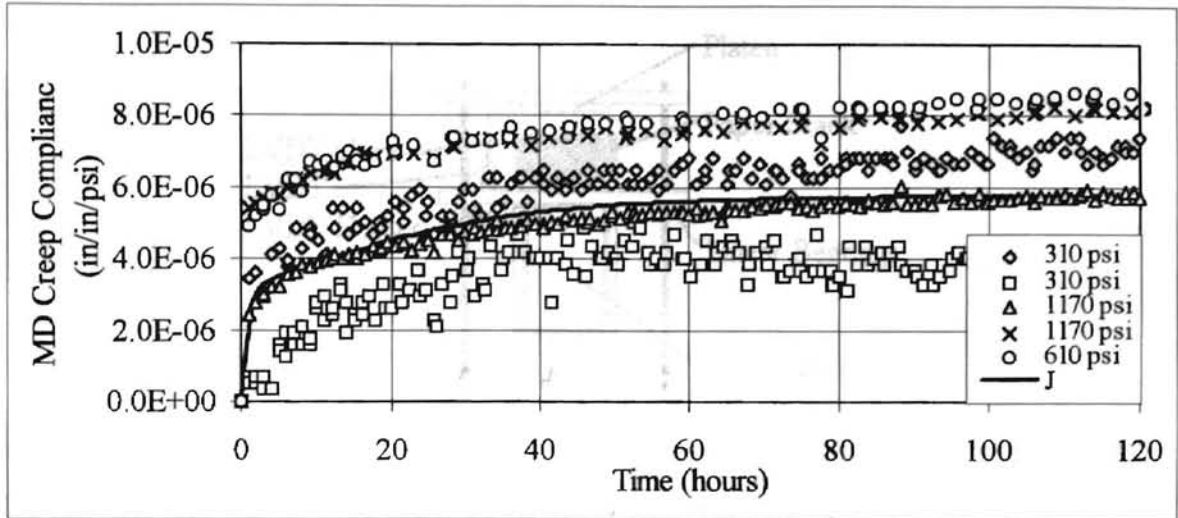
Figure 3.10. MD Creep Compliance for Newsprint for Various Stress Levels.

J_0	5.770E-06		
J_1	-1.835E-05	τ_1	5.427E+04
J_2	1.583E-05	τ_2	4.860E+04
J_3	-3.245E-06	τ_3	3.488E+03

Table 3.4. MD Creep Function Coefficients.

Radial Creep Measurements

The test setup is the same as used by Qualls [13] and is pictured below (Figure 3.11).

Figure 3.11. Radial Creep Test Setup.

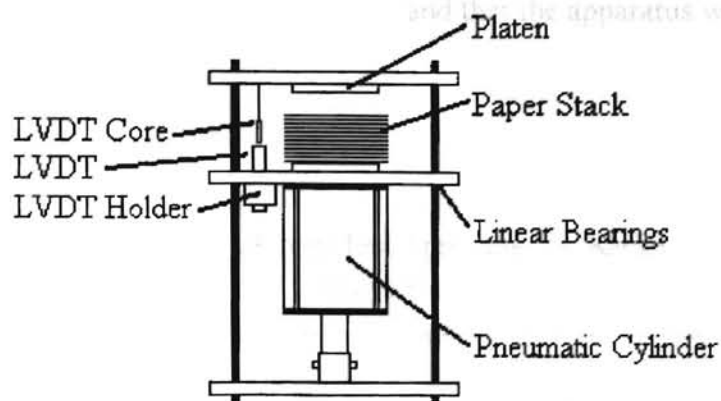Newsprint webs were cut into six-by six-inch squares, with sufficient squares to form a stack height of one inch. The stack was placed on the 4.25 inch diameter platen. Compressed nitrogen gas provides the pressure to move the 3.5 inch diameter cylinder. The required nitrogen pressure, given below, was measured by two inline pressure gauges with 5 psi graduations.

$$P_{Nitrogen} = P_{stach} \frac{A_{platen}}{A_{piston}} \tag{3.5}$$

The pressure was controlled by a regulator attached to the nitrogen tank. As the stack deforms a Trans-Tek #282 LVDT outputs a voltage that is acquired continuously by Labtech notebook. The LVDT has a 3.264 VAC/Inch/Volt input sensitivity and is linear over the range ±0.25 inches.

The reliability of the apparatus was tested by performing two radial modulus tests on the apparatus. Figure 3.12 shows how the results of the two tests compare to the radial modulus. Since the test results bracket the radial modulus, it is reasonable to

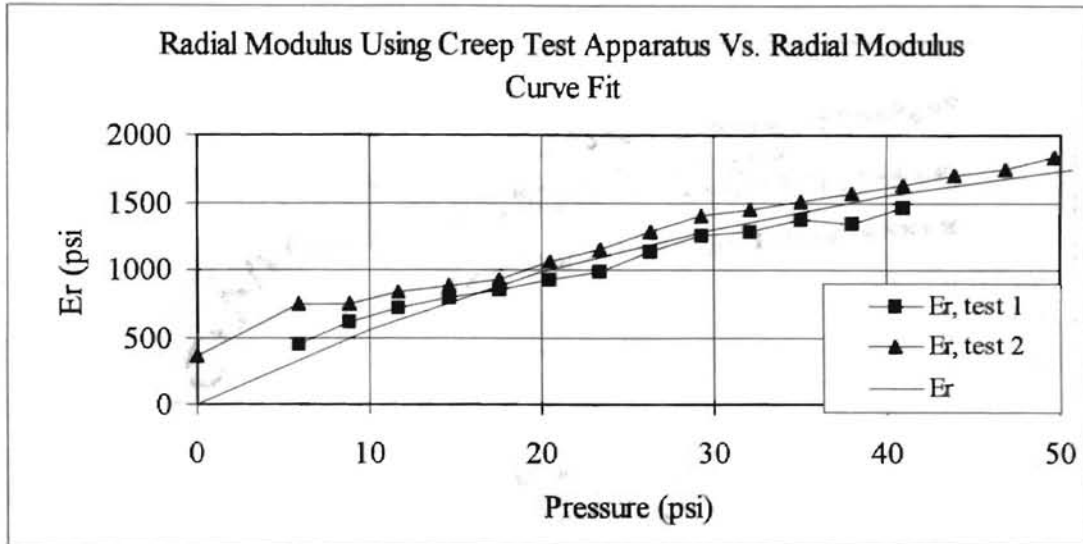assume that there is little sticking in the cylinder and that the apparatus will give reliable results.

Figure 3.12. Radial Modulus on Radial Creep Test Device.

Radial creep measurements were conducted at 57, 40, 23 and 10 psi levels. Qualls observed that the time dependent strain for LDPE was stress independent. This was clearly not the case for newsprint, as is shown in the Figure 3.13 (with the initial strain removed). An additional test was performed at 57 psi to check for repeatability. The separation of the two tests is an indication of the error or of the non-repeatability of this test. Using the separation of the two 57 psi curves as a percentage error aids in determining the nature of the response. Error bands for each stress level can be estimated by applying the percent error to each stress level. If the time dependent strain is

31

independent of stress, it would be expected that the error bands of each stress level would overlap. This is not the case.
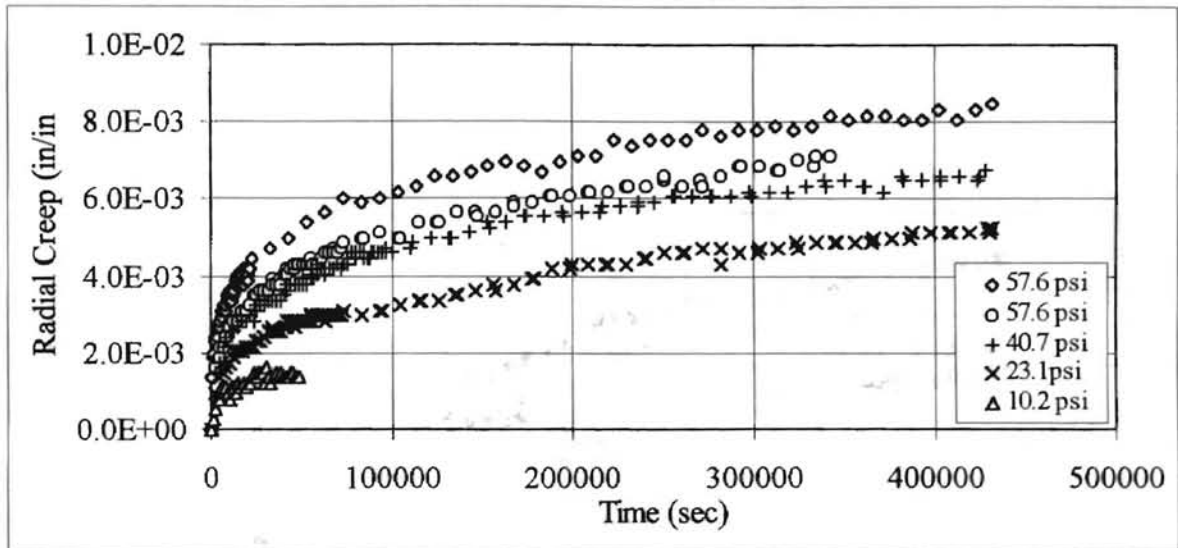

Figure 3.13. Radial Creep of Newsprint at 72°F and 45%RH for Various Stress Levels.

Figure 3.14 shows the error bands (as lines) for the 40 psi case. It can be clearly seen that the bands overlap the 50 psi and the 23 psi data points. To prevent overcrowding of the graph the error bands for the other stress levels were not included in Figure 3.14, but they clearly would overlap the 40 psi bands. This leads to the conclusion that the radial creep compliance is independent of stress. Therefore, radial coefficients for the generalized Maxwell model can be found using the same procedure as J_θ. That is, the radial compliance data was averaged at all stress levels. The resulting curve was fit to the general creep compliance form. The coefficients appear below in Table 3.5.

J_0	J_1	τ_1	J_2	τ_2
1.940E-4	-6.596E-5	3.592E+3	-1.281E-4	2.595E+5

Table 3.5. Coefficients of Radial Compliance.
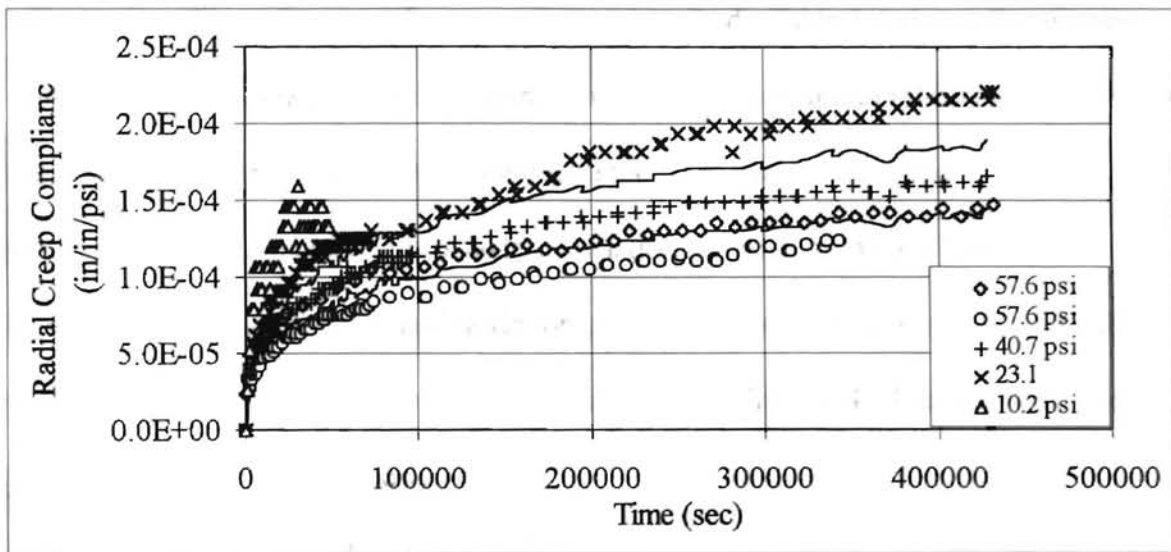
Figure 3.14. Radial Creep Compliance for Newsprint at 72°F and 45%RH for Various Stress Levels.

In-Roll Stress Measurement

Pull tabs are often used to measure the interlayer pressure in wound rolls. Pull

tabs used in this research were constructed of ½ inch wide by 0.001 inch thick stainless

steel feeler gauge surrounded by a brass shim stock sandwich. The ends of the gauges

were reinforced with tape to provide a gripping surface for the force transducer. Careful

33

handling of the pull tabs is required because foreign objects (like fingerprint oil) can effect the pull tab. Calibration is achieved by placing a known pressure, such as a weight, on a pull tab inserted in a stack of web material and then measuring the force required to just slip the gauge. This process is repeated at several stress levels covering the desired measurement range. A straight line fit can then be made of the calibration data. Each pull tab must be calibrated separately, as previously described. Table 3.6 shows the average calibration coefficients and standard deviation for all pull tabs used in this research. Qualls suggests using the calibration that is unique to the individual pull tab, and this author agrees. Therefore, the individual standard deviation for most of the pull tabs is significantly less than the standard deviation of 0.614. The significance of the pull tab calibration is not presented here but will be discussed in Chapter 4. The interlayer stress is found using the Equation below.

$$Pressure = a + Pull \ Force \times b \tag{3.6}$$

Pull tabs were placed at discrete points along the roll radius. The tabs were staggered circumferentially to minimize localized stress.

There are limitations to the use of pull tabs. As the interlayer pressure increases, so does the force required to slip the tab. As a result, pressure measurement is limited by the force transducer's maximum load, feeler gauge tensile strength and even the physical strength of the operator. Pull tabs in this study were calibrated to 30 psi.

	Average	Standard Deviation
a	0.332	0.614
b	0.571	0.045

Table 3.6. Pull Tab Coefficients.

Viscoelastic Winding Properties

Newsprint rolls were wound at 600 psi and 750 psi. Pull tabs were inserted at 0.75, 1.25, 1.75, 2.25 and 2.75 inches away from the outer radius of the steel core. Since all creep tests were performed for five days, the roll measurement tests lasted five days. Four pulls were made per pull tab, alternating sides after every pull. This method of measurement allowed the pull tabs to stay centered in the roll. The results of these four measurements were averaged and the experimental values compared to those produced by the winding model in the Figures 3.15-3.18. Table 3.7 shows the parameters input into Viscowinder. The * indicates that the winding stress is the wound on tension.

Winding Stress*	500 or 645 psi	**Roll Inside Radius**	1.6875in.
Modulus of Core Material **Poisson's ratio**	30e6 psi 0.3	**Roll Outer Radius**	5.1875 in.
Core Inner Radius	1.4875 in	**Caliper**	2.8 mils

Table 3.7. Additional Parameters to Viscowinder.

As mentioned previously, tension loss occurs in centerwinding of newsprint rolls. Qualls' viscoelastic model does not handle tension loss. As a result, the initial stress distribution output by Viscowinder is much higher than what was measured. The WHRC (Web Handling Research Center) has produced a program called Winder that predicts the initial stress distribution in wound rolls. Winder can model tension loss by using the modified Hakiel model.

Winder has been shown to accurately predict the initial stress distributions in wound rolls. It is no surprise that the tension loss model utilized via Winder agreed with the initial radial stresses measured in this thesis. This confirms that tension loss is occurring and that the pull tab measurements are valid (Chapter 4 expands on the meaning and significance of the pull tab measurements). Winder can also predict the initial radial stress states that exists in a roll not experiencing tension loss (by using the non-modified Hakiel model). The Hakiel model predictions can be made to agree with the tension loss predictions by changing the winding stress input into the Hakiel model. This final winding

stress is the wound on tension that is then input into Viscowinder as the winding stress. The wound on tension produced by Winder appears in Table 3.7.

In Figures 3.15 and 3.16 the lines represent the output of Viscowinder. The heaviest lines correspond to time zero. Time progresses from top to bottom. Viscowinder was run at the same times that experimental data was taken. For example, in Figure 3.15 the second line from the top represents output from Viscowinder after 3600 seconds have passed, the third line is from Viscowinder at 7200 seconds, and so on.
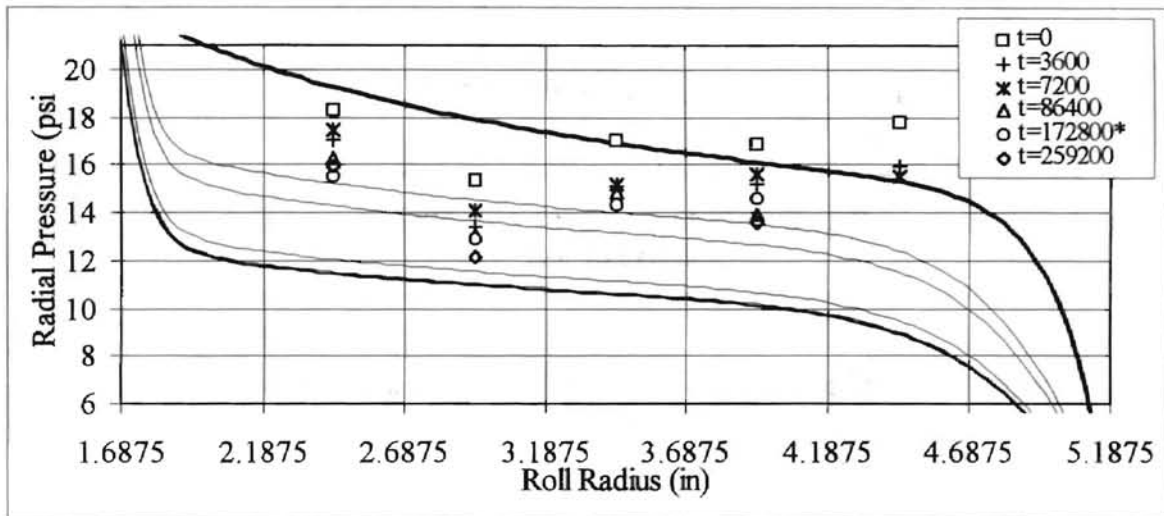

Figure 3.15. Experimental Results of Winding Newsprint at 600 psi Compared to Viscowinder Prediction.

There were five pull tabs used in the roll represented in Figure 3.15. However, two pull tabs broke during the course of the experiment and no additional data could be taken at those particular radii. The roll was stored in the environmental chamber at the conditions listed at the start of this chapter. However, the refrigeration system developed a leak and conditioning was lost (at 172800* seconds). This did not seem to greatly

effect the relaxation, which can be seen by the proximity of the last data points to the lowest line (at 259200 seconds). This is probably due to the small change in humidity that the loss of temperature caused (humidity was 48%RH and the temperature was 82°F after conditioning loss). After temperature control was lost this test was halted.
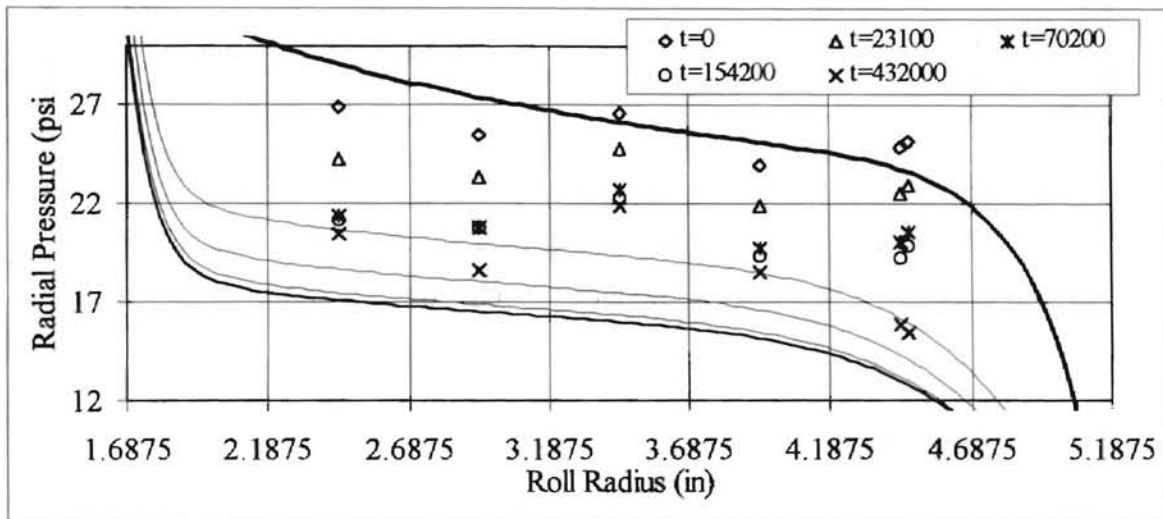

Figure 3.16. Experimental Results of Winding Newsprint at 750 psi Compared to Viscowinder Prediction.

Because of the problems encountered another winding test was run, but this time at a higher tension (Figure 3.16).

It appears from Figures 3.15 and 3.16 that Viscowinder predicts more relaxation than was actually measured. Table 3.6 indicates that the pull tabs, in general, have nearly ±01 psi calibration offset indicating that the decay measured in Figure 3.15 may be nonsensical. However, this is an offset and not an indication of the sensitivity of the pull tab. Each pull tab has an offset that remains constant throughout the experiment. Chapter 4 examines the measurement errors. The following two graphs indicate how each

38

individual point decayed over time. It is not clear from Figures 3.17 and 3.18 if the roll may still be relaxing beyond the test time period.
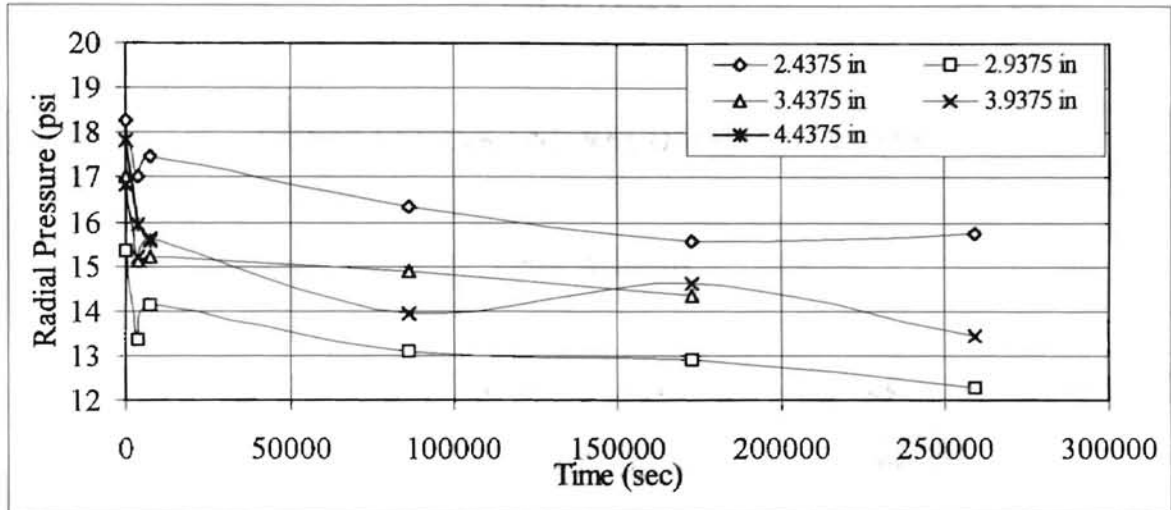

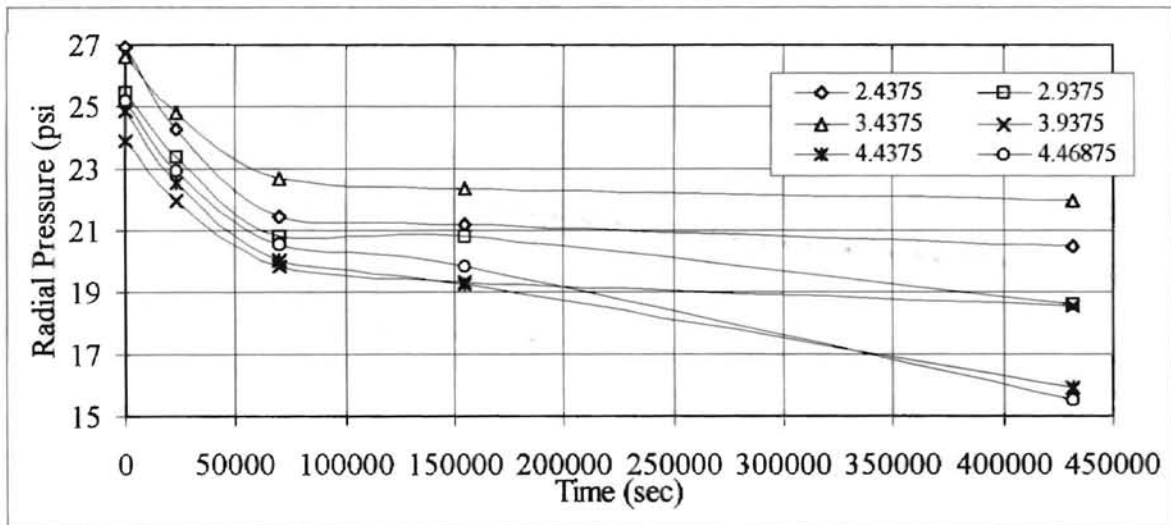Figure 3.17. Decay of Radial Pressure of Newsprint Wound at 600 psi.

Figure 3.18. Decay of Radial Pressure of Newsprint Wound at 750 psi.

CHAPTER 4

CONCLUSIONS AND RECOMMENDATIONS

Error Analysis

An estimate of the error of the test procedure can be made using Viscowinder.

Recall from Chapter 3 that the J_θ and J_r coefficients were formed from all the dispersed

data. By fitting new J_θ and J_r curves to the upper and lower extremes of the radial and

MD creep compliance data, it can be shown that the error in Viscowinder's prediction is

about $\pm 15.4\%$ or ± 2.4 psi (Figures 4.1 and 4.2)
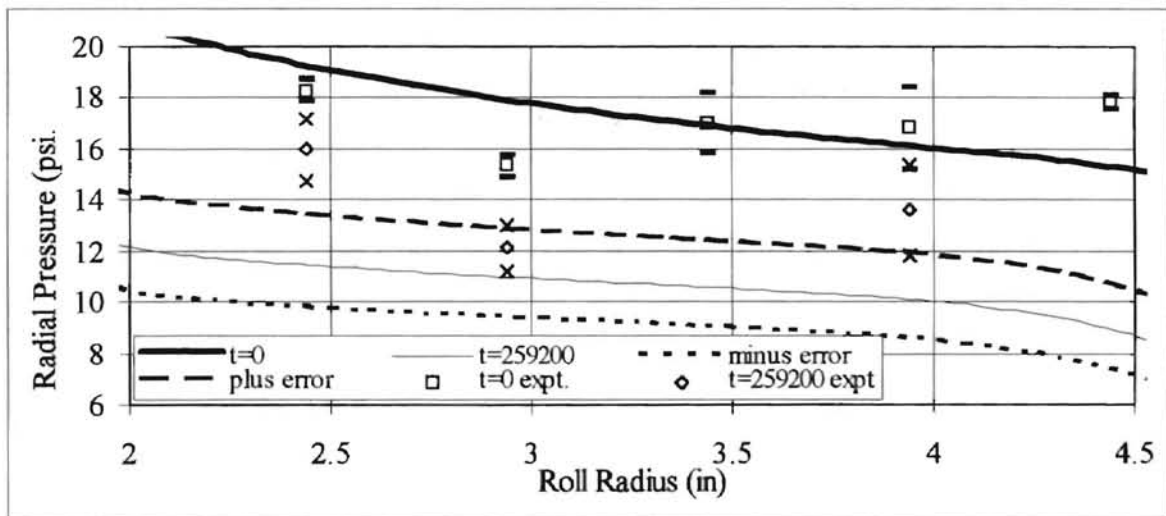

Figure 4.1. Error in Creep Compliance Test and Pull Tabs Demonstrated on the 600 psi Wound Roll.

The lower three lines in Figure 4.1 represent the upper and lower ranges to the 259200 second line. For example, the minus error line comes from fitting the respective creep compliance curves through the upper bounds of the dispersed data. The t=259200 second line is the output of Viscowinder using the compliance coefficients found in Chapter 3. The next line up (plus error) represents the fit through the lower bounds of the dispersed data. Additionally, Figure 4.1 shows the standard deviation of each individual pull tab at time zero and at time 259200 (represented by a pair of - or + bracketing the data point).
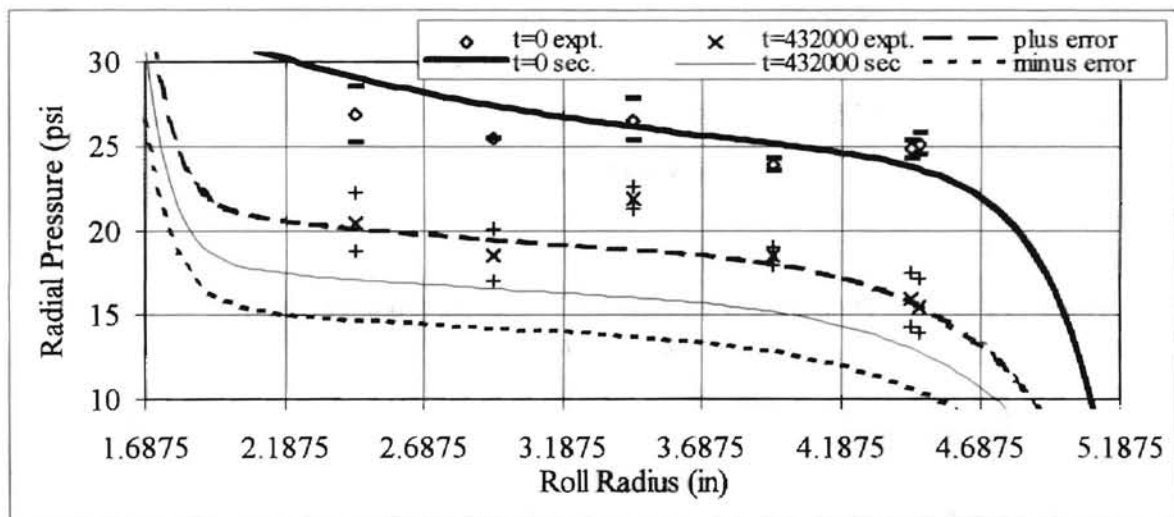
Figure 4.2. Error in Creep Compliance Test and Pull Tabs Demonstrated on the 750 psi Wound Roll.

Figures 4.1 and 4.2 demonstrate that Viscowinder correctly predicts the relaxation of newsprint rolls, given the error in the measurements. The error in the pull tabs (± 1.2 psi on average including both calibration and measurement) indicates that the compliance coefficients from Chapter 3 do an adequate job of modeling the viscoelastic behavior.

However, it appears from both figures that the plus error line does a much better job of modeling the newsprint roll. Figure 4.3 shows how Figure 3.16 would look if the radial and MD compliance coefficients were the same as those used to create the plus error curve in Figures 4.1 and 4.2.
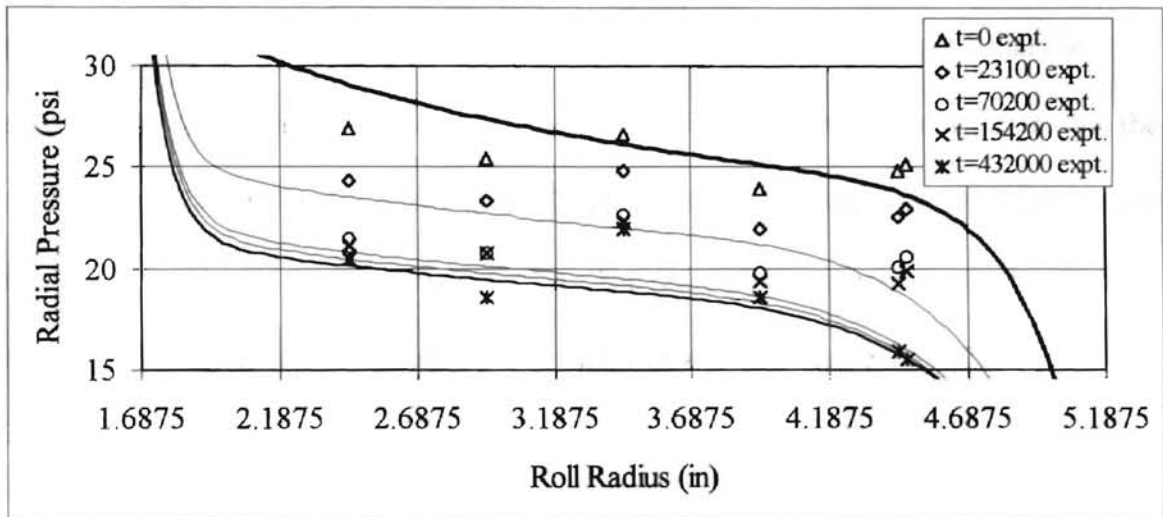
Figure 4.3. 750 psi Wound Newsprint Roll with Lower Bounds used to Form Creep Compliances.

Why does the plus error curve do a better job? First of all, Qualls commented that the radial compliance did not greatly effect his model. In fact, he suggested that, if some error was acceptable, then J_r could be taken to be zero. This is verified in Figure 4.4 (the difference in the two lower lines is 0.5 psi). This means that J_θ is more likely the source of the variation. The most difficult property to measure and understand is the thickness of newsprint. While it is not clear how thickness actually effects the stress in the web, it is clear how thickness effects the calculation of the compliance and the MD modulus. Recall

that the creep compliance is the time dependent strain divided by the initial stress. The initial stress that the web experiences is:

$$Stress = Force/(width\ of\ web)*(web\ caliper) \qquad (4.1)$$

An error in web caliper of ± 0.1 mil translates into an error of $\pm 3.57\%$ for the compliance and an error of $\pm 3.7\%$ for the MD modulus. When applied to Viscowinder, the error due to thickness is $\pm 7.3\%$ per 0.1 mils. It was shown in Chapter 3 that the thickness ranged from 3 to 2.6 mils with the average being 2.8 mils. Put another way, the thickness was 2.8 ± 0.2 mils. A swing of 0.2 mils means Viscowinder will produce a result that is within $\pm 14.6\%$ (compared to 15.4%). The reason the top error line better predicts the viscoelastic response is because the average web caliper is more likely 2.6 mils than it is 2.8 mils.
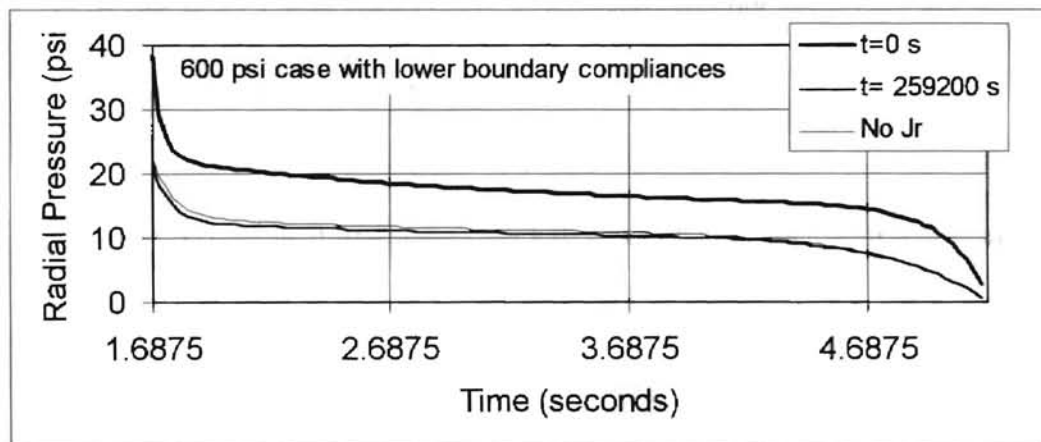

Figure 4.4. Output of Viscowinder taking J_r to be Zero.

Conclusions

The following conclusions can be drawn from this research:

1. Viscowinder is versatile enough to correctly predict the viscoelastic nature of newsprint.

2. The MD and radial creep compliances for newsprint are stress independent.

3. When centerwinding newsprint tension loss occurs, care must be taken to find the radial modulus and the wound on tension. The wound on tension can then be input into Viscowinder as the winding stress.

4. The error of Viscowinder was found to be ±2.4 psi, which was mainly due to the difficulty in correctly measuring the web's caliper. Additionally, the pull tabs used to measure the radial pressure were accurate to within ±1.2 psi.

5. A rise in 10°F and 3% RH over a twenty-seven hour period did not seem to greatly effect the winding results.

6. It was verified that it would be reasonable to take the radial creep compliance to be zero while introducing only a 0.5 psi error for the room temperature relaxation studied. However, this may not be reasonable for cases in which the temperature and moisture content are changed.

Future Work

Why was the thickness of newsprint so difficult to measure? One factor may have been the slight difference in humidity of the storage chamber and the test area. It was stated in Chapter 2 that changing humidity leads to a change in thickness. Since the rolls

44

were conditioned at 45%RH and thickness was measured at 50-55%RH, it is reasonable that changes in thickness due to humidity changes showed up in the thickness measurements. Changes in humidity also effect the modulus and the deformation of newsprint. An investigation into the effects of changing humidity on thickness, modulus and strain that can be added to Viscowinder would greatly boost the power and usefulness of the Qualls model.

However, certain difficulties will be encountered in modeling the hygroscopic behavior of paper. It was stated that temperature and humidity effects are interchangeable. This does not mean that the two act independently of one another. As the temperature increases it lowers the moisture content of the paper and lowers the glass transition temperature. In effect, a higher temperature means less moisture is needed to see a change in material properties. How much less moisture will be needed? Is it proportional to the rise in temperature? The study would have to account for changes in moisture content at specific temperatures and relative humidities. Additionally, an increase in the moisture content will increase the deformation of the web. It can be envisioned that at some point the radial compliance will be large enough that it cannot be ignored. However, the circumferential compliance should increase proportionally such that it dominates the model, and hence, changes in the radial modulus can be ignored. That is, the radial compliance will be small compared to the circumferential compliance. How does moisture content effect the viscoelastic response? These questions must be answered in order to model the hygroscopic nature of newsprint. Unfortunately, it may take a paper specialist to answer them.

BIBLIOGRAPHY

[1]   Altmann, H.C. *Formulas for Computing the Stresses in Center-Wound Rolls.*
        Tappi Journal Vol. 51, No. 4. Pp. 176-179. April 1968.

[2]   Brezinski, J.P. *The Creep Properties of Paper.* Tappi Journal Vol. 39, No. 2. Pp.
        116-128. 1956.

[3]   Byrd, Van L.. *Effect of Relative Humidity Changes During Creep on Handsheet
        Paper Properties.* Tappi Journal Feb. 1972 Vol. 55 No. 2. Pp. 247-252.

[4]   Findley, W., J. Lai. and K. Onaran. *Creep and Relaxation of Nonlinear
        Viscoelastic Materials.* North-Holland Publishing Co. New York. 1976.

[5]   Giachetto, R.M., J.K. Good and J.D. Pfeiffer. *Losses in Wound on Tension in the
        Centerwinding of Wound Rolls.* AMD Vol. 149, Web Handling. ASME 1992.
        Pp. 1-12.

[6]   Gutterman R.P. *Theoretical and Practical Studies of Magnetic Tape Winding
        Tensions and of Environmental Toll Stability.* Contract No. DA18-119-SC-42
        (1959). General Kinetics, Inc. Arlington VA.

[7]   Hakiel, Z. *Nonlinear Model for Wound Roll Stresses.* Tappi Journal Vol. 70 No.
        5. Pp. 113-117. May 1987.

[8]   Haslach, Henry W. Jr. *Mechanics of Moisture Accelerated Tensile Creep in
        Paper.* Tappi Journal Vol.77 No. 10. Pp. 134-140.

[9]   Lin, J.Y. and R.A. Westmann. *Viscoelastic Winding Mechanics.* Journal of
        Applied Mechanics Vol. 56. Pp. 821-827. Dec. 1989

[10]   Pfeiffer, J.D. *Internal Pressures in a Wound Roll.* Tappi Journal Vol. 49 No. 8.
        Pp. 342-347. Aug. 1966.

[11]   Pfeiffer, J.D. *Measurement of the K2 factor of Paper.* Tappi Journal Vol. 64 No.
        4. Pp. 105-105. April 1981.

[12]   Pfeiffer, J.D. *An Update to Pfeiffer's Roll-Winding Model.* Tappi Journal Vol.
        70 No. 10. Pp. 130-131. Oct. 1987.

[13]   Qualls, W. *Hygrothermomechanical Characterization of Viscoelastic
        Centerwound Rolls.* Ph.D. Dissertation. Oklahoma State University. May 1995.

[14]   Roisum, David R. *Moisture Effects on Webs and Rolls*. TAPPI Vol. 76 No. 6. Pp. 129-136.

[15]   Salmén, L. *Responses of Paper Properties to Changes in Moisture Content and Temperature*. Transaction of the Fundamental Research Symposium. Oxford: September 1993.

[16]   Salmén, N.L. and Ernst L. Back. *Moisture-Dependent Thermal Softening of Paper, Evaluated by its Elastic Modulus*. TAPPI Vol. 63, No. 6. Pp. 117-120.

[17]   Skowronski, J. P. Lepoutre, and W. Bichard. *Measuring the Swelling Pressure of Paper*. TAPPI Vol. 71 No. 7. Pp. 125-130.

[18]   Tramposch, H. *Relaxation of Internal Forces in a Wound Reel of Magnetic Tape*. Journal of Applied Mechanics Vol. 32 No. 4. Pp. 865-873. Dec. 1965.

[19]   Tramposch, H. *Anisotropic Relaxation of Internal Forces in a Wound Reel of Magnetic Tape*. Journal of Applied Mechanics. Pp. 888-894. Dec. 1967.

[20]   Urbanik, Thomas J.. *Hygroexpansion-Creep Model for Corrugated Fiber Board*. Wood and Fiber Science 27(2) 1994 pp. 134-140.

[21]   Urbanik, Thomas J.. *Swept Sine Humidity Schedule for Testing Cycle Period Effect on Creep*. Wood and Fiber Science 27(1) 1995 pp. 68-79.

[22]   Yagoda, H.P. *Resolution of Core Problem in Wound Rolls*. Journal of Applied Mechanics Vol. 47. Pp. 847-854. Dec. 1980.

VITA

Samuel David Price

Candidate for the Degree of

Master of Science

Thesis: VISCOELASTIC RELAXATION OF NEWSPRINT IN WOUND ROLLS

Major Field: Mechanical Engineering

Biographical:

Education: Graduated from Lawton High School, Lawton, Oklahoma in May 1990; received Bachelor of Science Degree in Mechanical Engineering from Oklahoma State University, Stillwater, Oklahoma in May 1995.
Completed requirements for Master of Science degree with a major in Mechanical Engineering at Oklahoma State University in December 1996.

Experience: As an undergraduate was employed by Oklahoma State University Department of Residential Life as a Residential Assistant (1991-1993); employed by OPSEIS, Inc. in the summer of 1993 as an engineering intern; worked various part-time service related jobs while working for undergraduate degree (1993-1995); employed by Oklahoma State University Department of Mechanical Engineering as an undergraduate and as a graduate research assistant (1995-present); served as a teaching assistant at Oklahoma State (1995-present).

Professional Memberships: Pi Tau Sigma, National Mechanical Engineering Honor Society, Engineer Intern in the State of Oklahoma.